applied sciences

MDPI

Article

Impact Characteristics of a Bidirectional Pneumatic DTH Hammer for Unconsolidated Formations

Yuanling Shi [1,2,*], Shuang He [2] and Conghui Li [2]

[1] Academician Workstation in Anhui Province, Anhui University of Science and Technology, Huainan 232001, China
[2] School of Earth and Environment, Anhui University of Science and Technology, Huainan 232001, China; 2022200006@aust.edu.cn (S.H.); 2021200002@aust.edu.cn (C.L.)
* Correspondence: ylshi@aust.edu.cn

Abstract: With advantages of high efficiency and low cost, DTH hammer drilling has been highly applied in various drilling projects. When drilling in unconsolidated formations, it is prone to drilling accidents such as drilling tools sticking or burying. Thus, a bidirectional pneumatic DTH hammer is designed to drill boreholes using forward impact and release sticking drilling tools using backward impact. With a floating gas distribution mechanism, impact strokes of the DTH hammer piston can be changed when flat keys are in a different position of the key grooves on the gas distribution shaft. In drilling mode, the piston has a larger impact stroke and can impact the anvil at high speeds to drive the bit breaking rocks. When drilling tools become stuck, by changing to a smaller impact stroke, the piston can impact backward on the gas distribution valve to break rocks above the DTH hammer so sticking drilling tools can be released. According to the structure and working principle of the bidirectional pneumatic DTH hammer, a physical model based on the pneumatic transmission circuit is established; then, a simulation model is built with pneumatic transmission module components in software of SimulationX 4.1 student version. Piston velocities, displacements, and impact energy are analyzed, with main factors including piston mass, total weight of the DTH hammer, compressed air pressure, and backward impact stroke being considered. Analysis results show that working characteristics of the DTH hammer are fairly affected by piston mass and compressed air pressure. Based on the changing laws of the impact frequency, peak of impact velocity, and impact energy, a piston mass of 18 kg, total weight of 125 kg, gas source pressure of 2.2 MPa, and lifting distance of 60 mm for backward impact were recommended. To verify the performance of the bidirectional pneumatic DTH hammer, field experiments were carried out in the gravel stratums. The bidirectional DTH hammer was in good working condition and the maximum drilling rate can reach up to 1.5 m/min. By lifting the DTH hammer away from the bottom of the borehole and pumping compressed air, the DTH hammer piston could achieve a high frequency backward impact. There are no drilling tools' sticking or burying accidents in the drilling experiments. The bidirectional pneumatic DTH hammer can effectively drill boreholes in loose formations and deal with drilling tools' sticking or burying accidents.

Keywords: pneumatic DTH hammer; unconsolidated stratum; bidirectional impact; piston speed; impact energy

check for updates

Citation: Shi, Y.; He, S.; Li, C. Impact Characteristics of a Bidirectional Pneumatic DTH Hammer for Unconsolidated Formations. *Appl. Sci.* **2023**, *13*, 11797. https://doi.org/10.3390/app132111797

Academic Editor: Tiago Miranda

Received: 5 September 2023
Revised: 20 October 2023
Accepted: 25 October 2023
Published: 28 October 2023

Copyright: © 2023 by the authors. Licensee MDPI, Basel, Switzerland. This article is an open access article distributed under the terms and conditions of the Creative Commons Attribution (CC BY) license (https://creativecommons.org/licenses/by/4.0/).

1. Introduction

In drilling projects, unconsolidated formations like the sand layer, gravel bed, and cobbles formation are regarded as one of the most complex and challenging formations to deal with [1–3], since it is prone to causing drilling accidents such as drilling tools sticking, drilling tools burying, and borehole collapse. Once drilling tools are stuck or buried in unconsolidated formations, retrieving them from boreholes is almost impossible, which will incur additional time and cost consumption [4–6]. In order to drill boreholes

successfully in unconsolidated formations, casing while drilling finds increasing utilizations recently, including long spiral rotary drilling with casing and percussive rotary drilling with casing [7,8]. In the literature [9], a risk analysis to Casing-while-Drilling (CwD) programs was carried out to highlight its technical benefits and a modeling approach was presented for applying risk analysis to CwD to achieve successful drilling programs. Pinlu Cao and colleagues utilized an orthogonal experimental method to study a drill bit for CwD and investigated the influence of bit parameters on reverse circulation performance [10]. Pablo. G. Cirimello et al. presented a fractographic analysis and failure analysis of K55 seamless casings used for drilling an oil well with the method of CwD and recommended large-grained tube steels in conjunction with high-quality premium connections to enhance the durability of the casings for withstanding repeated torque and compression stresses [11]. In the literature [12], drilling-with-casing (DwC) equipment for a water well was introduced and newly developed Down-the-Hole (DTH) hammers for DwC were studied, which exhibit higher impact energy. In the literature [13], CwD technology was proven to be the most effective solution against borehole instability in the Sultanate of Oman, where Fiqa formation was present. Bo et al. [14] designed a drill bit for reverse circulation DTH hammer drilling with casing to pass through complicated formation, and impact of drill bit gas channel structural parameters on reverse circulation performance was then studied using a combination of numerical simulations and experimental analysis. Compared with conventional drilling methods, CwD can effectively reduce drilling cost and time consumption. However, this method has its flaws. Firstly, the process of CwD is complex, and on the other hand, due to the friction between the casings and borehole wall, drilling depth by this method is limited.

With advantages of high efficiency, low cost, safety, and reliability, DTH hammer drilling has found extensive application in oil and gas drilling, mineral exploration, geological exploration, and foundational engineering construction [15–17]. According to the actuating medium, DTH hammers can be divided into two classes: hydraulic and pneumatic [18–20]. Since air is used as the circulating medium, there is no environmental pollution in pneumatic DTH hammer drilling and drilling fluids leakage can be avoided in loose and unconsolidated formation. Dae Ji Kim et al. [21] formulated a dynamic model for a DTH hammer and analyzed its operational characteristics, so as to enhance the impact efficiency of the DTH hammer by optimizing design parameters and suggesting modifications. In the literature [22], computational fluid dynamics (CFD) were adopted to evaluate the performance of RC-DTH air hammers and the effects of parameters such as rebound coefficient, input air pressure, and piston mass were thoroughly examined. In the literature [23], a pneumatic dynamic model for a DTH hammer and a motion model for a drill bit were established, and then these two models were combined to assess impact efficiency under varying rock conditions. Aiming at breaking into rocks with reduced weight on the bit and lower power, and to also remove rock cuttings effectively, Yinchao Wang et al. [24] designed a rotary-percussive ultrasonic drill and employed modal analysis to finely adjust the resonance frequencies of both its percussive unit and rotary unit. For increasing drilling efficiency, DTH air hammers were developed with curvilinear free surfaces piston in the literature [25] to impact rocks with the minimum energy input using no contact between the pistons with hammer bodies. In the literature [26], a large diameter reverse circulation DTH hammer was designed to improve the penetration rate during rescue well drilling, which was used to deal with underground coal mine disasters. Although the air DTH hammer has achieved good drilling results in different types of borehole drilling projects, when it is used in loose and unconsolidated layers, accidents like drilling tools sticking or burying are still inevitable to occur, which will cause damage to drilling tools and scrapping of boreholes.

In order to leverage the advantages of DTH hammer drilling and deal with accidents of drilling tools sticking or burying in unconsolidated formations, a bidirectional pneumatic DTH hammer is proposed in this paper. During the drilling process, the bidirectional pneumatic DTH hammer breaks rocks and drills boreholes with forward impact, while

when drilling tools become stuck in boreholes, the DTH hammer can help to release drilling tools using backward impact. To study the impact characteristics of the bidirectional DTH hammer, optimize its structure, and verify the rationality of its designed functions, a simulation method and field experiment will be applied. The paper is organized as follows: in the second part of this paper, the configuration of the bidirectional pneumatic DTH hammer is stated in detail. Then, a theoretical model and a simulation model of the bidirectional DTH hammer are constructed based on its structure and pneumatic transmission theory. Impact characteristics of the DTH hammer are studied as its piston impacts forward and backward in the fourth section. And lastly, drilling experiments are conducted to validate the operational effectiveness of the DTH hammer.

2. Configuration of the Bidirectional DTH Hammer

Figure 1 illustrates the bidirectional pneumatic DTH hammer. It is composed of a drill bit, a bit joint, an anvil, a gas distribution sleeve, an outer cylinder, a piston, an inner tube, an inner cylinder, a gas distribution valve, an upper shaft sleeve, a gas distribution shaft, a check valve, an inner joint, a pipe joint, and other components. The components that achieve bidirectional impact are installed in the outer cylinder. The main parameters for the DTH hammer are listed in Table 1.

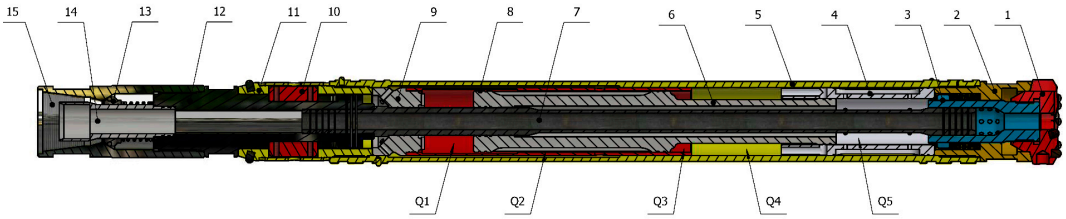


Figure 1. Configuration of the bidirectional DTH hammer. 1. drill bit, 2. bit joint, 3. anvil, 4. gas distribution sleeve, 5. outer cylinder, 6. piston, 7. inner tube, 8. inner cylinder, 9. gas distribution valve, 10. flat key, 11. upper shaft sleeve, 12. gas distribution shaft, 13. check valve, 14. Inner joint, and 15. pipe joint.

Table 1. Main parameters of the DTH hammer.

Parameters	Value
Diameter of the drill bit	135 mm
Diameter of the outer cylinder	130 mm
Length of the DTH hammer	1861 mm
Impact energy of single stroke	Forward: 500–900 J Backward: 300–450 J
Impact frequency	10–16 Hz
Piston mass	16–20 kg
Impact stroke	200–230 mm
Nominal pressure of the gas source	1.0–1.4 MPa
Nominal flow rate of the gas source	10–20 m^3/min

The component for achieving bidirectional impact is the floating gas distribution mechanism, which is composed of a pipe joint, an inner joint, an O-ring seal, a check valve, a check valve spring, a gas distribution shaft, carbide teeth, two shaft keys, an upper shaft sleeve, a gas distribution valve, an inner tube, and an outer cylinder, as shown in Figure 2. The upper end of the floating gas distribution mechanism is connected to dual-wall drill pipes via its pipe joint using trapezoidal threads, where driving torque and axial force (pressure or tension) can be obtained from drilling rigs. The lower end of the pipe joint is connected to the gas distribution shaft with threads. There are two key grooves on the gas distribution shaft, where two flat keys are mounted. The upper shaft sleeve is connected with the outer cylinder of the DTH hammer via threads, and there are also two key grooves

on the upper shaft sleeve. Two flat keys are mounted between the gas distribution shaft and the upper shaft sleeve to achieve torque transmission. The length of the key grooves on the gas distribution shaft is the sum of the length of the flat keys and the designed floating stroke, while the length of the key grooves on the upper shaft sleeve is consistent with the length of the flat keys. The piston of the DTH hammer is driven to reciprocate using compressed air. When the flat keys are in a different position of the key grooves on the gas distribution shaft, the impact stroke of the piston will change.

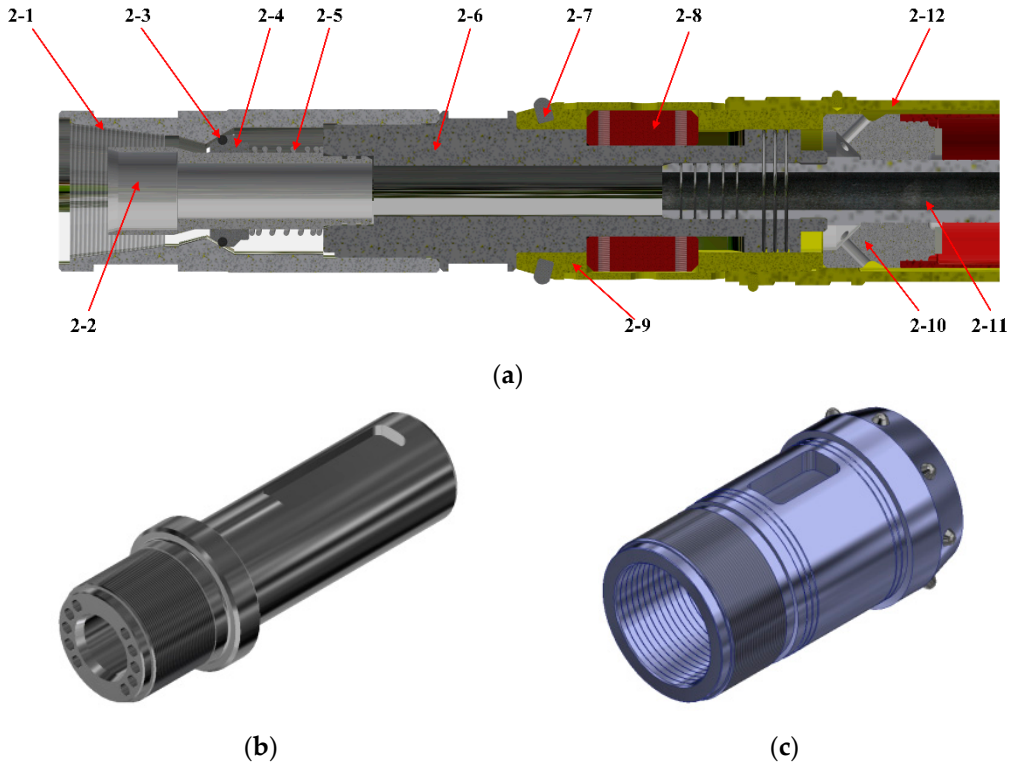


Figure 2. Structure of floating gas distribution mechanism. (**a**) Floating gas distribution mechanism; (**b**) gas distribution shaft (2-6); and (**c**) upper shaft sleeve (2-9). 2-1. pipe joint, 2-2. inner joint, 2-3. O-ring seal, 2-4. check valve, 2-5. Check valve spring, 2-6. gas distribution shaft, 2-7. alloy teeth, 2-8. shaft key, 2-9. upper shaft sleeve, 2-10. gas distribution valve, 2-11. inner tube, and 2-12. outer cylinder.

Different impact strokes for the piston will be applied when the DTH hammer is used for drilling boreholes using forward impact and releasing sticking drilling tools using backward impact. In drilling mode, the flat keys are located at the upper end of the key grooves on the gas distribution shaft and the piston has a larger impact stroke. It means that the piston can descend with a sufficient acceleration process and then impact the anvil at high speeds to drive the bit to break rocks. Afterwards, the piston runs upward in the direction opposite to its initial speed. Since there is also a sufficient deceleration stroke, when the piston ascends to the gas distribution valve, its end velocity is very small or even zero, ensuring that the piston only has an impact on the drill bit to achieve impact drilling and does not impact drill pipes to protect the reliability of drill pipe connections. When drilling tools become stuck, by lifting drill pipes, the gas distribution shaft moves upward relative to the upper shaft sleeve and then the inner tube moves upward. In such cases, the flat keys are located at the lower end of the key grooves on the gas distribution shaft and the piston has a smaller impact stroke. And thus, when the piston runs backward close to the gas distribution valve, it still has a high final speed, thereby achieving impacts on the gas distribution valve. Then, the upper shaft sleeve breaks rocks and soils above the DTH hammer with its alloy teeth, so sticking drilling tools can be released from boreholes.

3. Bidirectional Impact Model for the Pneumatic DTH Hammer

3.1. Theoretical Model

Due to structure of the piston and outer cylinder, the DTH hammer is divided into several different gas chambers, as shown in Figure 1, which is the chamber above the piston (Q1), the chamber between the inner cylinder and the piston (Q2), the chamber between the inner spacer ring and the piston (Q3), the chamber between the gas distribution sleeve and the piston (Q4), and the chamber below the piston (Q5). The reciprocating motion of DTH hammer piston directs the compressed gas into different chambers. The piston serves as more than just a power component for producing impact energy; it also functions as a control element for regulating its own reciprocating motion. This reciprocating motion is an intricate and dynamic process. During a complete impact process of the piston, the chamber above the piston (Q1) undergoes two gas admissions, two gas emissions, one expansion process, and one compression process; the chamber between the inner cylinder and piston (Q2) maintains a constant connection with the high-pressure air source; the chamber between the inner spacer ring and piston (Q3) and the chamber between the gas distribution sleeve and piston (Q4) connect constantly, which undergoes two gas admissions, two gas emissions, one expansion process, and one compression process too; and the chamber below the piston (Q5) is constantly connected to the low pressure air in boreholes.

Taking gas in the chamber above the piston (Q1) for example, at the beginning of the piston downward impact, the chamber Q1 is connected to the high pressure air source, which is in a compressed air admission state. Afterwards, the connection between chamber Q1 and the high-pressure gas source gradually closes with the DTH hammer piston moving forward. When chamber Q1 is disconnected from the high-pressure air source, the volume of chamber Q1 gradually increases due to the forward motion of the piston, and thus, compressed air expands to do work. The piston proceeds to descend and impacts the anvil ultimately to achieve impact drilling, during which process, chamber Q1 will be connected to the low pressure gas in boreholes and the gas in chamber Q1 will be discharged. After the piston impacts the anvil, the direction of the piston movement changes from forward to backward. In the initial stage of backward movement, chamber Q1 is still connected to low pressure gas in the borehole, and it is still in the state of exhaust. After being disconnected from the low pressure gas in the borehole, chamber Q1 is in a sealed state. As the piston moves backwards, the volume of chamber Q1 decreases and the air inside the chamber is compressed. With the piston moving backwards continuously, chamber Q1 gradually connects with the high-pressure air source again, and this is the second time high pressure air enters chamber Q1, causing a deceleration motion with the increasing acceleration in the piston's motion.

According to the working principle of a bidirectional DTH hammer, it is essentially a pneumatic transmission system. The reciprocating motion of the DTH hammer piston inside the DTH hammer is exactly the same as a piston operating in an air cylinder. However, the switching of the gas direction in the DTH hammer is achieved by changing the relative position between the piston and the DTH hammer cylinder. For a pneumatic transmission system, directional valves are used to change the intake and exhaust status of air cylinders. Based on the structure of the bidirectional pneumatic DTH hammer, a physical model was constructed, as shown in Figure 3. There were also five chambers from the left to right, which are Q1, Q2, Q3, Q4, and Q5, respectively. For the DTH hammer, the opening and closing of each chamber is determined using the piston position. In the pneumatic transmission circuit model, the connection between the above chambers and high pressure air source or low pressure air in boreholes can be changed by controlling the opening and closing of valves.

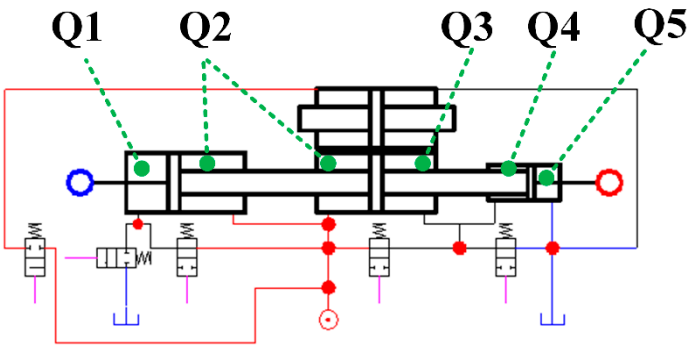


Figure 3. Pneumatic transmission model of the bidirectional DTH hammer.

3.2. Simulation Model

During DTH hammer drilling, the piston is driven by compressed air moving forward and backward alternately, which is a complex dynamic process with nonlinear characteristics. It is difficult to obtain an analytical solution via theoretical analysis. To study the dynamic characteristics of the DTH hammer, a dynamic simulation model was established using SimulationX 4.1 student version according to the pneumatic transmission physical model built in Section 3.1, as shown in Figure 4. In the pneumatic module of the SimulationX software, pneumatic components such as cylinders and valves are available. In the simulation model, the pneumatic DTH hammer is divided into four parts, which are the DTH control part (Area I), the dynamic testing part (Area II), the hammer functional part (Area III), and the rock interaction part (Area IV), respectively. In the control part (Area I), position feedback control functions are adopted to output control signals via logical operation by measuring the displacement of the DTH hammer cylinder and piston and then control the opening and closing of air supply valves and exhaust valves dynamically. The dynamic testing part (Area II) is used to measure parameters in the reciprocating motion of the piston, such as displacement, velocity, acceleration, force, and collision. In the DTH hammer functional part (Area III), four cylinders are adopted as the actuator of the DTH hammer and their dimensions are defined based on the structure of the piston, inner cylinder, gas distribution sleeve, and inner tube. By setting a different piston diameter and cylinder dimeter, the five chambers of the DTH hammer (Q1, Q2, Q3, Q4, and Q5) are built. These actuators are driven by compressed air and their working status depends on the position signals' output from the control part. In the rock interaction part (Area IV), the interaction between the DTH hammer and rocks is simulated using a spring damper and a mass block.

What is more, in the simulation model, the four cylinders are rigidly connected. The mass of outer cylinders and pistons are represented by one mass block, respectively. Thus, the working mechanism of these cylinders is consistent with the real DTH hammer.

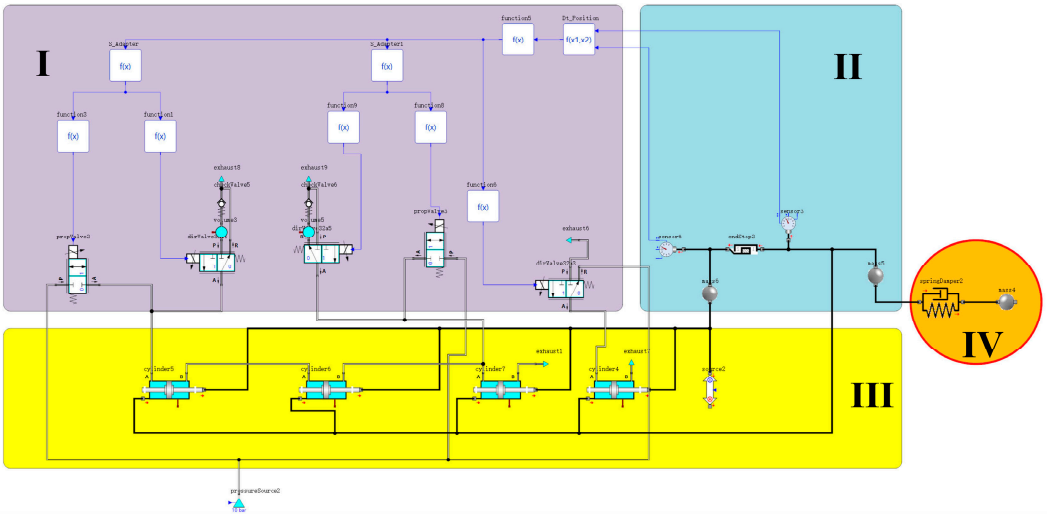


Figure 4. Simulation model of the DTH hammer based on SimulationX. Area I. DTH control part, Area II. the dynamic testing part, Area III. the hammer functional part, Area IV. the rock interaction part.

4. Result Analysis and Discussion

4.1. Impact Characteristics under Different Piston Mass

Setting the mass of the piston to 16 kg, 18 kg, and 20 kg respectively, when the piston stroke is 230 mm, the piston velocity is obtained as shown in Figure 5 using the simulation model established in Section 3. With a piston mass of 16 kg, an impact frequency of 15 Hz is generated. In the first impact cycle, the peak of impact velocity can reach up to 10.15 m/s. Due to friction occurring between the piston and the cylinder during the reciprocating movement, the peak velocity of the piston tends to diminish. As a result, there is a 2.76 m/s difference between the highest and lowest velocity peaks within a one-second timeframe. When the piston mass is 18 kg, the impact frequency is 14 Hz. In the first impact cycle, the peak of impact velocity can reach up to 9.54 m/s. There is also a decreasing trend in the piston velocity peak and its decrease within 1 s is 2.19 m/s. When the piston mass is 20 kg, the impact frequency is 13 Hz. In the first impact cycle, the peak of impact velocity can reach up to 9.02 m/s. The peak velocity decrease within 1 s is 2.21 m/s. According to the above results, when the piston's mass increases, both the impact frequency and the peak velocity decrease.

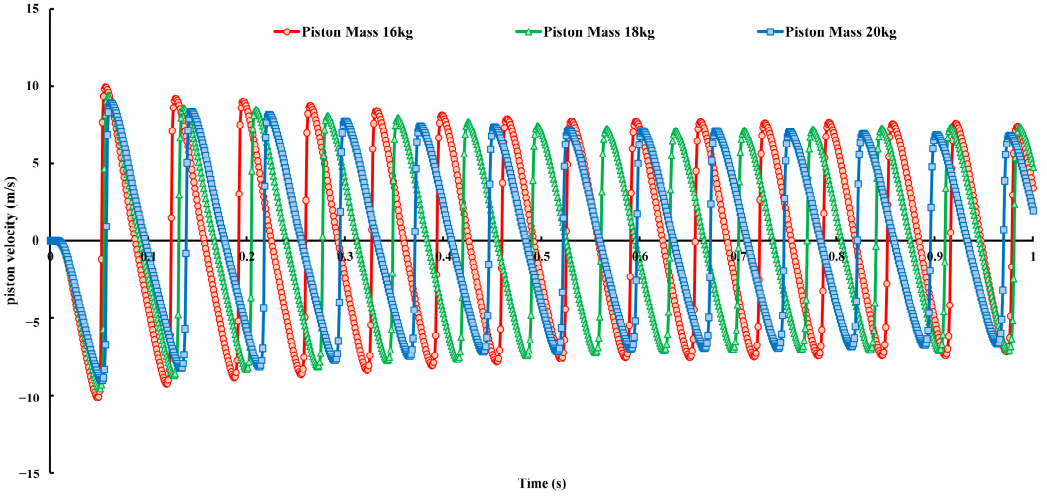


Figure 5. Piston velocity at different piston mass.

When the DTH hammer acts on rocks, there are displacements for cylinders and pistons in the simulation calculation. To analyze the displacement variation in the piston, displacement difference between pistons and cylinders is taken as the target parameter. The piston's initial position in the simulation is at the top of its impact stroke, close to the gas distribution valve and farthest from the anvil. Displacement difference between the piston and the outer cylinder is displayed in Figure 6, when the piston masses are set to 16 kg, 18 kg, and 20 kg, respectively. From the curve, it can be seen that for the piston with a mass of 16 kg, it descends 227 mm from its initial position to impact the anvil and then returns upwards. The upper endpoint is 29 mm away from the initial position. Afterwards, the next impact process begins. With the separation between the upper endpoint and the initial position, it can avoid impacting on the DTH hammer pipe joint, thereby protecting the reliability of the threaded connection between the DTH hammer and drill pipes. It is worth noting that due to friction between the pistons and cylinders, there is an increasing tendency in the separation between the upper endpoint and the piston's initial position. Within 1 s, the separation can be up to 84 mm. For the piston with a mass of 18 kg, it descends 227 mm from its initial position to impact the anvil and then returns upwards. The upper endpoint is 26 mm away from the initial position. There is also an increasing trend in the separation between the upper endpoint and the initial position, and the separation can be up to 71 mm within 1 s. In the simulation for the piston with a mass of 20 kg, the piston descends 227 mm from its initial position and then returns upwards. The upper endpoint is 24 mm away from the initial position. There is also an increasing trend in the distance between the upper endpoint and the initial position. Within 1 s, the distance can be up to 72 mm. Drawing from the aforementioned findings, it can be concluded that as the piston mass increases, the separation between the upper endpoint and the piston's initial position decreases.

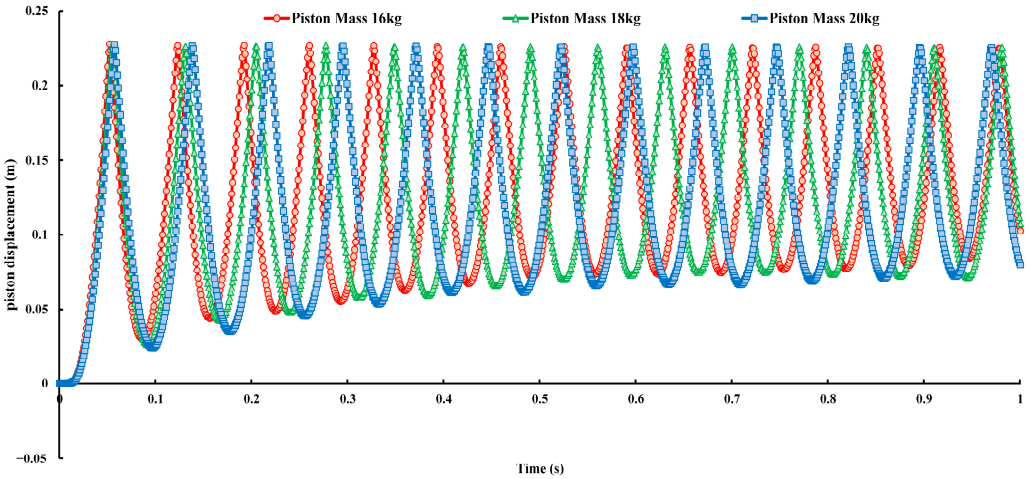


Figure 6. Piston displacement with different piston mass.

Figure 7 shows the piston impact energy when the piston mass of the DTH hammer is set to 16 kg, 18 kg, and 20 kg. respectively. To facilitate the analysis of the piston impact energy, it is defined that when the piston velocity is positive, the impact energy is also positive; and conversely, as the piston velocity is negative, the impact energy is negative. For the piston with a mass of 16 kg, when the piston descends and impacts the anvil for the first time, it can generate impact energy with a value of 824 J. Afterwards, due to the decrease in the piston's final velocity, there is a trend of decreasing in impact energy. When the piston has a mass of 18 kg and descends to the anvil, the first impact can generate impact energy with a value of 819 J. When the piston mass is 20 kg, the first impact can generate impact energy with a value of 814 J. From the above analysis, it can be seen that minor changes in the piston mass do not substantially affect the piston's impact energy.

Based on the above analysis results of the impact frequency, peak of impact velocity, and impact energy, the recommended piston mass is 18 kg.

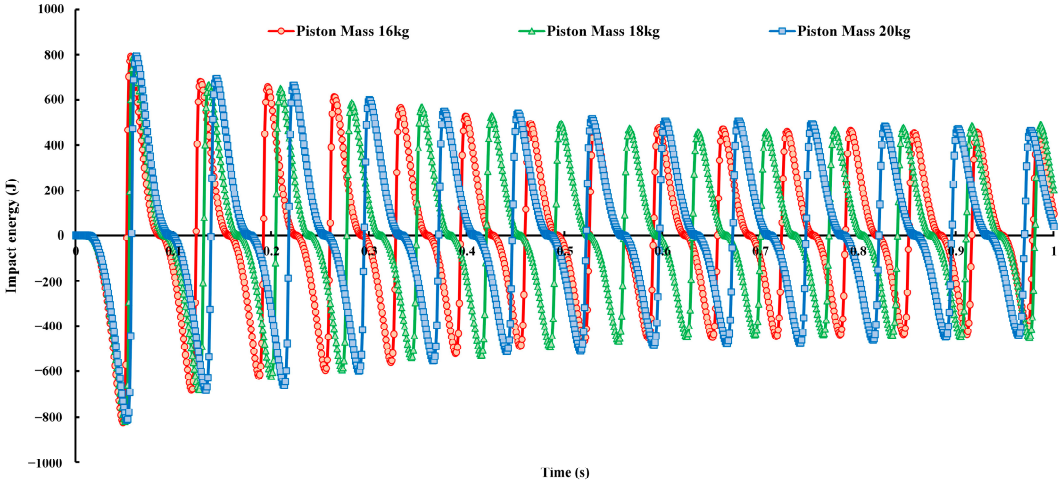


Figure 7. Impact energy with different piston mass.

4.2. Total Weight of DTH Hammer

When the mass of the piston is set to 18.66 kg and the total weight of the DTH hammer is set to 125 kg, 150 kg, and 175 kg, respectively, piston velocity is shown in Figure 8. As the total weight of the DTH hammer is 125 kg, 150 kg, and 175 kg, respectively, piston impact frequencies are all 13.5 Hz, while the peaks of impact velocity within the first impact cycle are 9.22 m/s, 9.37 m/s, and 9.37 m/s. The analysis results indicate that with a constant piston mass, the total weight of the DTH hammer has a negligible influence on both the piston's impact frequency and its peak impact velocity. However, increasing the total weight of the DTH hammer will increase the demand for the drilling rig lifting capacity and workload of DTH hammer transportation. Therefore, on the premise of insuring function and strength of the DTH hammer, it should minimize the total weight as much as possible.

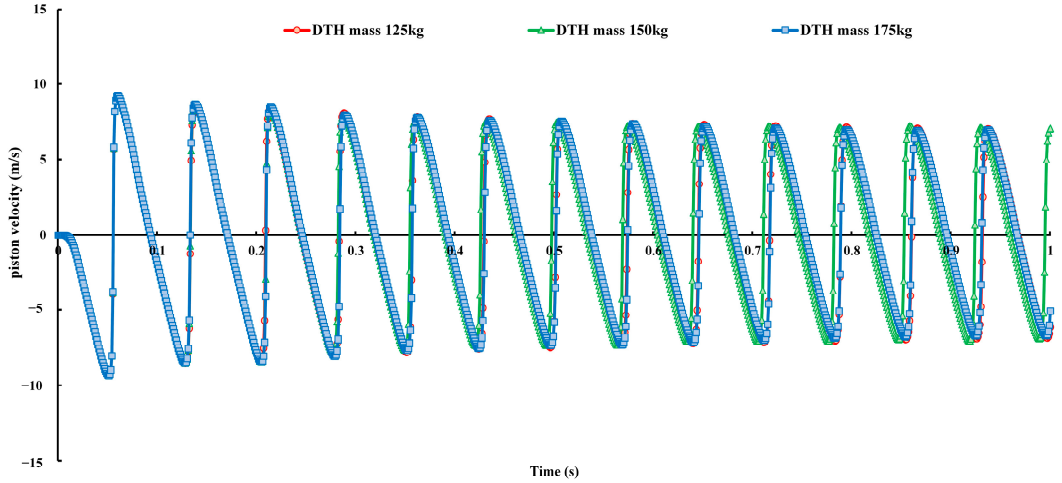


Figure 8. Piston velocity at different DTH hammer weight.

Figure 9 is the displacement difference curve between the piston and outer cylinder when the piston mass is 18.66 kg and the total weight of the DTH hammer is 125 kg, 150 kg, and 175 kg, respectively. From the curve, it can be seen that when the total weight of the DTH hammer is 125 kg, the piston descends 227 mm from the initial position to impact its anvil and then returns at an upward speed until it reaches to the upper endpoint, which is 26 mm away from the initial position. Within a 1 s simulation, the distance between the

upper endpoint and the initial position can reach up to 74 mm. When the total weight of the DTH hammer is 150 kg, the piston descends 227 mm from the initial position to impact its anvil and returns upwards too, until it reaches the upper endpoint with a distance of 26 mm from the initial position. Within 1 s of simulation, the distance can reach up to 75 mm. When the total weight of the DTH hammer is 175 kg, the piston descends 227 mm from the initial position to impact its anvil and returns upwards too, until it reaches the upper endpoint with a distance of 26 mm from the initial position. Within 1 s of simulation, the distance can reach up to 76 mm. According to the results, it can be seen that the total weight of the DTH hammer has little effect on piston displacement.

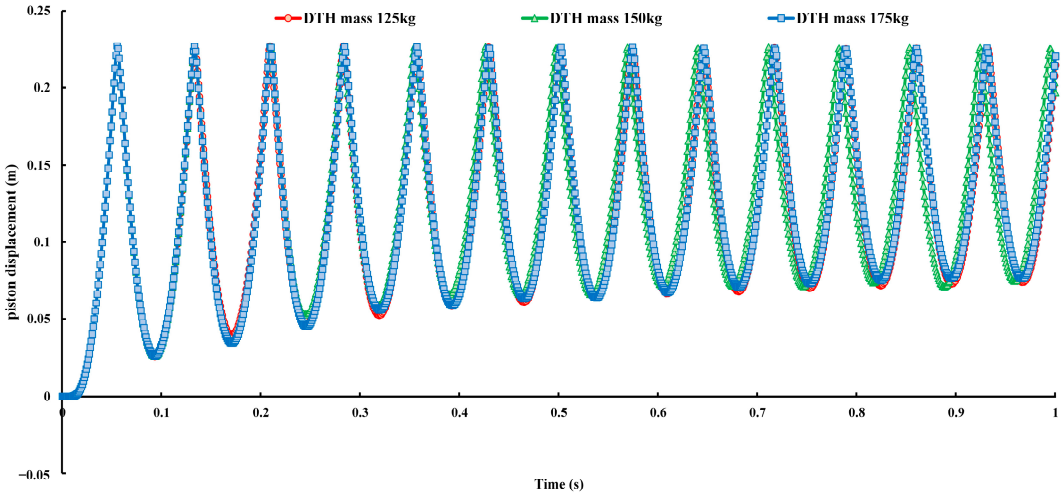


Figure 9. Piston displacement with different DTH hammer total weight.

Figure 10 shows the piston impact energy when the piston mass of the DTH hammer is 18.66 kg and the total weights of the DTH hammer are set to 125 kg, 150 kg, and 175 kg, respectively. For the DTH hammer with a total weight of 125 kg, when the piston first descends and impacts the anvil, it can generate impact energy with a value of 818 J. When the DTH hammer has a weight of 150 kg, the piston's first impact can generate impact energy with a value of 818 J. When the DTH hammer total weight is 175 kg, the first impact can generate impact energy with a value of 818 J. From the above analysis, it can be seen that variations in the total weight of the DTH hammer do not significantly affect the piston's impact energy. Based on the above analysis results of the impact frequency, peak of impact velocity, and impact energy, the recommended total weight is 125 kg.

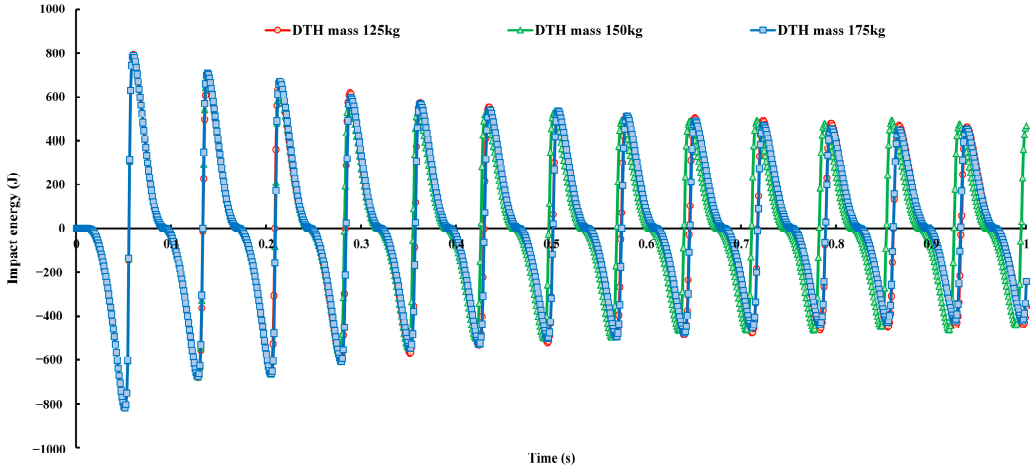


Figure 10. Impact energy with different DTH hammer total weight.

4.3. Pressure of the Gas Source

One of the paramount factors influencing the drilling efficiency of the DTH hammer is pressure of the gas source. For the DTH hammer with a piston mass of 18.66 kg and a total weight of 128 kg, setting the gas source pressures to 2.0 MPa, 2.2 MPa, and 2.4 MPa, the piston velocity is shown in Figure 11. When the gas source pressure is 2.0 MPa, the impact frequency is 13.25 Hz. In the first impact cycle, the peak of impact velocity can reach up to 9.37 m/s. The peak impact velocity of the piston shows a declining trend, with a 2.45 m/s difference between the highest and lowest peaks within a one-second interval. When the gas source pressure is set at 2.2 MPa, the impact frequency measures 14.25 Hz. Within the first impact cycle, the peak impact velocity can reach up to 9.95 m/s, and there is a decreasing trend in the peak impact velocity, with a decreasing amplitude between the maximum peak and minimum peak of 2.61 m/s. When the gas source pressure is 2.4 MPa, the impact frequency is 14.25 Hz. Within the first impact cycle, the peak impact velocity can reach up to 9.95 m/s, and there is a decreasing trend in the peak impact velocity, with a decreasing amplitude of 2.61 m/s. From the analysis results, it is evident that as the gas source pressure rises, the piston's impact frequency, peak of impact velocity, and velocity reduction amplitude all increase. To enhance the piston's peak impact velocity during the drilling process, it is advisable to adjust the gas source pressure accordingly.

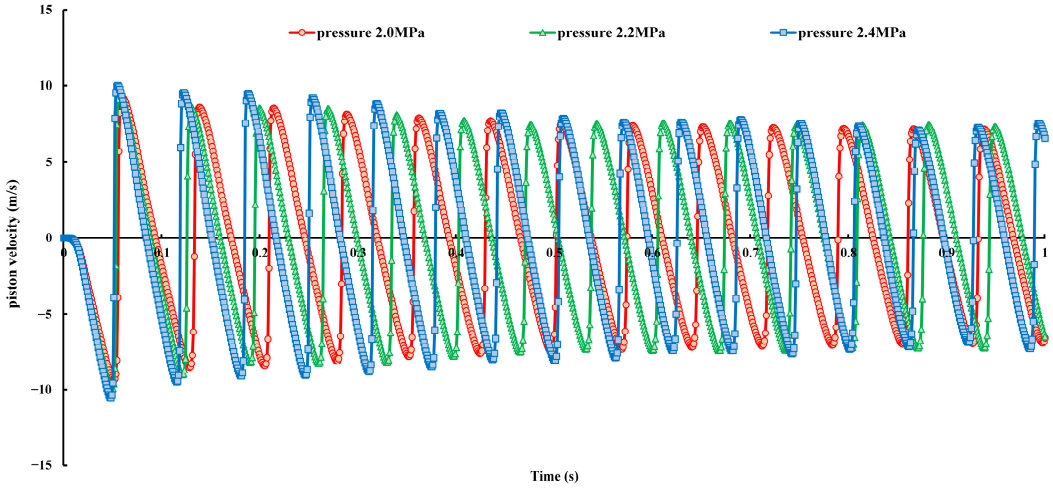


Figure 11. Piston velocity at different gas source pressure.

In Figure 12, the displacement curve between the piston and cylinder of the DTH hammer is depicted. This is illustrated for three different scenarios: when the piston mass is 18.66 kg, the total DTH hammer weight is 128 kg, and the gas source pressures are set at 2.0 MPa, 2.2 MPa, and 2.4 MPa, respectively. Observing the curve, it becomes evident that at a gas source pressure of 2.0 MPa, the piston descends 227 mm from the initial position to impact its anvil and then returns upward to the upper endpoint with a distance of 25 mm from the initial position. Within 1 s of simulation, the above distance can reach up to 72 mm. When the gas source pressure is 2.2 MPa, the piston descends 227 mm from the initial position to impact its anvil and then returns upward to the upper endpoint with a distance of 31 mm from the initial position. Within 1 s of simulation, the above distance can reach up to 77 mm. When the gas source pressure is 2.4 MPa, the piston descends 227 mm from the initial position to impact its anvil and then returns upward to the upper endpoint with a distance of 38 mm from the initial position. Within 1 s of simulation, the above distance can reach up to 77 mm. As indicated by the curve, it is apparent that the gas source pressure has very little influence on the displacement of the piston, which is determined using the structure of the DTH hammer. As the pressure of the gas source increases, the upper endpoint of the piston increases. This is because the upward movement of the piston changes the gas distribution direction of the high pressure

gas inside the DTH hammer. When the piston ascends to the position where high pressure gas is supplied to the upper chamber, increasing the gas source pressure means causing resistance to the upward movement of the piston. As the piston decelerates and reaches the point of zero velocity during its upward movement, it will be further away from the initial position.

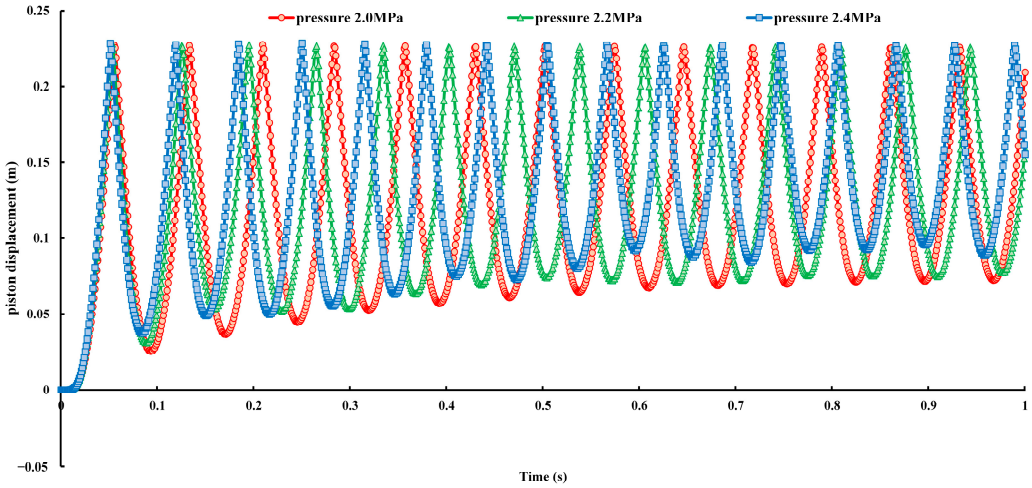


Figure 12. Piston displacement at different gas source pressure.

Figure 13 shows the piston's impact energy when the gas source pressures are 2.0 MPa, 2.2 MPa, and 2.4 MPa, respectively. When the air source pressure are 2.0 MPa, 2.2 MPa, and 2.4 MPa, the first impact of the piston can generate impact energy with a value of 818 J, 923 J, and 1029 J. In other words, when the piston mass is constant, an increase in gas source pressure can increase the piston peak impact velocity, thereby increasing the piston impact energy. Based on the above analysis results of the impact frequency, peak of impact velocity, and impact energy, the recommended gas source pressure is 2.2 MPa.

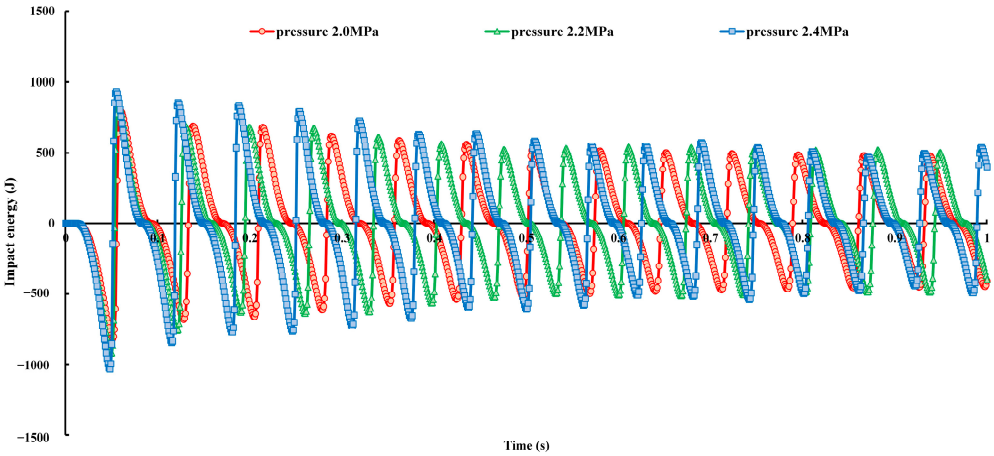


Figure 13. Impact energy at different gas source pressure.

4.4. Backward Impact Stroke

During drilling process, the piston backward movement stroke can be changed by lifting the inner tube assembly of the DTH hammer, thereby achieving a backward impact. In order to rescue drilling tools successfully in the case of sticking or burying accidents, the piston must have sufficient upward impact energy in the upward impact process. For a DTH hammer with its piston mass of 18.66 kg and total weight of 128 kg, when the lifting distance of its inner tube assembly is set to 40 mm, 50 mm, and 60 mm, respectively, the piston velocity is shown in Figure 14. When the lifting distance is 40 mm, the impact

frequency is 14.50 Hz and the peak impact velocity during the first impact cycle can reach up to 9.89 m/s. When the lifting distance is 50 mm, the impact frequency is 14.25 Hz and the peak impact velocity during the first impact cycle can reach up to 10.00 m/s. When the lifting distance is 60 mm, the impact frequency is 14.75 Hz and the peak impact velocity during the first impact cycle can reach 10.11 m/s. From the analysis results, it can be seen that as lifting distance increases, peak impact velocity increases, which is due to the forward distance of the piston increasing, thereby increasing the acceleration distance. When switching to the backward impact by lifting the inner tube, the piston still has relatively high downward end velocities, which is determined using the mechanism of the DTH hammer. Currently, the structure of the DTH hemmer cannot achieve zero forward impact end velocity.

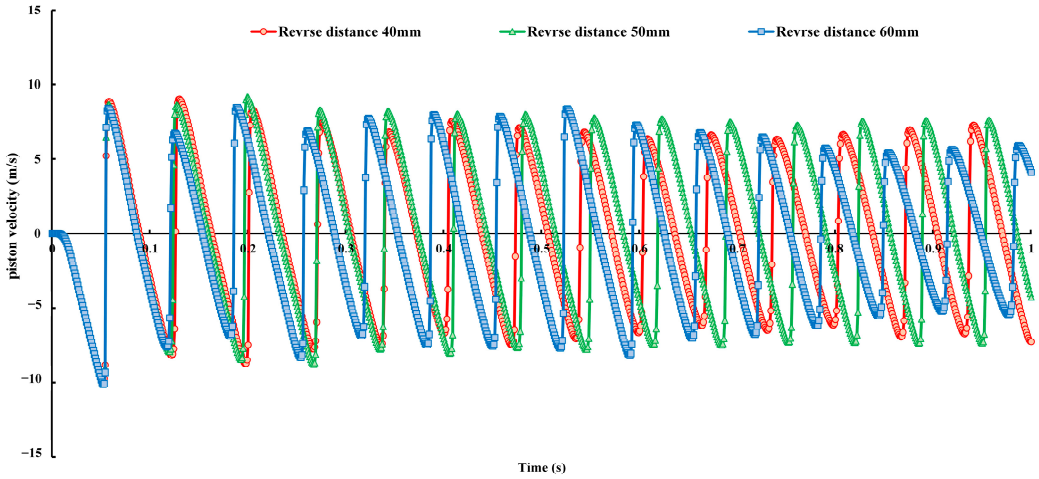


Figure 14. Piston velocity at different inner tube assembly lifting distance.

Figure 15 shows the displacement differences curve between the piston and outer cylinder when the lifting distances are 40 mm, 50 mm, and 60 mm, respectively. From the curve, it can be seen that when the lifting distance is 40 mm, the piston descends 227 mm from the initial position to impact its anvil and then returns upward to the upper endpoint with a distance of 52 mm from the initial position. Within 1 s of simulation, the above distance can reach up to 82 mm. When the lifting distance is 50 mm, the piston descends 227 mm from the initial position to impact its anvil and then returns upward to the upper endpoint with a distance of 62 mm from the initial position. Within 1 s of simulation, the above distance can reach up to 87 mm. When the lifting distance is 60 mm, the piston descends 227 mm from the initial position to impact its anvil and then returns upward to the upper endpoint with a distance of 73 mm from the initial position. Within 1 s of simulation, the above distance can reach up to 112 mm. As the lifting distance of the inner tube assembly increases, during the piston's deceleration and ascent to the point where its velocity reaches zero, it will progressively move farther away from its initial position.

Figure 16 shows the piston impact energy when the inner tube assembly is lifted upward with a different distance. As the lifting distances are 40 mm, 50 mm, and 60 mm, the first impact of the piston can generate impact energy with a value of 912 J, 935 J and 955 J. According to the results, when the piston mass is constant, an increase in the backward distance for the inner tube can increase the piston peak impact velocity, thereby increasing the piston impact energy. Based on the above analysis results of the impact frequency, peak of impact velocity, and impact energy, the recommended lifting distance for the backward impact is 60 mm.

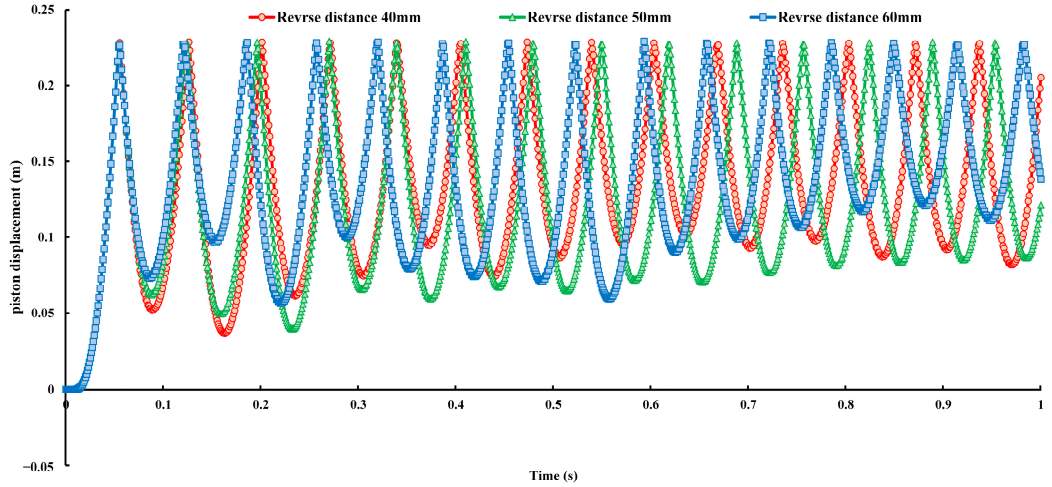


Figure 15. Piston displacement at different inner tube assembly lifting distance.

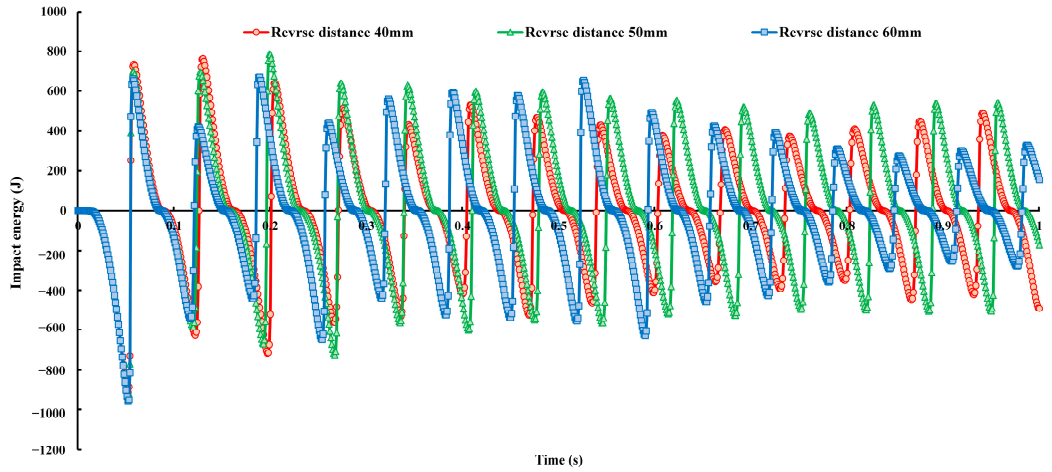


Figure 16. Impact energy at different inner tube assembly lifting distance.

5. Field Experiment of Pneumatic Bidirectional DTH Hammer

A set of DTH hammers was manufactured and field experiments were conducted in a gravel formation of Sichuan Province, so as to verify its working performance. The pneumatic bidirectional DTH hammer drilling experiments were conducted in a deep excavation of Chengdu Haifu Commercial Center, Kehua Middle Road, Chengdu, Sichuan Province, China. The strata in the area where the foundation pit is located from top to bottom is the Quaternary Holocene artificial fill layer (Q_4^{dl+mL}), the ice water accumulation cohesive soil layer of Quaternary middle lower Pleistocene (Q_{1+2}^{fgl}), and mudstone of Cretaceous Guankou formation (K_2^{g}). The Quaternary artificial fill layer is a miscellaneous fill with a thickness of about 0.8 m to 3.5 m at the upper strata. The lower part of the Quaternary artificial fill layer is a plain fill and mainly composed of cohesive soil with a loose structure, whose thickness is about 1.4 m to 3.8 m. For the ice water accumulation cohesive soil layer of the Quaternary middle lower Pleistocene, the upper strata is clay with a layer thickness of about 12.8 m to 14.4 m, in which a small amount of pebbles is contained. The lower part of the Quaternary middle lower Pleistocene is a pebble-containing cohesive soil with a layer thickness of about 0.9 m to 2.8 m, which is mainly composed of granite and sandstone. The pebble particle size is about 50 mm to 150 mm, with some being even more than 200 mm, with a medium roundness and pebble content of about 50% to 60%. The mudstone of the Cretaceous Guankou formation is an extremely soft rock and argillaceous texture structure, which is mainly composed of clay minerals.

The drilling rig used in the field experiments was a YG-100A hydraulic rig for anchoring borehole construction, which was manufactured by Chengdu Jindi Prospecting Machinery Co., Ltd. (Chengdu, China) All movements of this drilling rig are hydraulically driven, with a drilling depth of 50 m to 150 m, a drilling diameter of 89 mm to 250 mm, and a motor power of 25 kW, as shown in Figure 17. The bidirectional pneumatic DTH hammer has an outer diameter of 130 mm. During the experiments, the bidirectional DTH hammer was in good working condition, achieving a high drilling rate. In fact, the maximum drilling rate can reach up to 1.5 m/min, and the actual bit on the bottom time was much shorter than the auxiliary time of adding drill pipes. By lifting the DTH hammer away from the bottom of the borehole and pumping compressed air, the DTH hammer piston can achieve a high frequency backward impact. To verify the function of releasing sticking drilling tools using a backward impact, an appropriate amount of rock cuttings was added to the borehole to simulate a drilling tools' sticking accident. Rock cuttings above the DTH hammer could be cleared away and the drill pipes and DTH hammer could be lifted out of the borehole smoothly. There are no drilling tools' sticking or burying accidents. The above results indicated that the bidirectional pneumatic DTH hammer can effectively form boreholes in loose formations and deal with drilling tools' sticking or burying accidents.



Figure 17. Field experiments.

6. Conclusions

To leverage the advantages of DTH hammer drilling and deal with accidents of drilling tools sticking or burying in unconsolidated formations, a bidirectional pneumatic DTH hammer was designed to drill boreholes using forward impact rotary drilling and retrieve sticking drilling tools from boreholes using a backward impact. A floating gas distribution mechanism was applied to change the impact stroke of the DTH hammer piston. With a larger impact stroke, the piston could impact the drill bit forward with high speeds to drill boreholes. While changing to a smaller stroke, the piston impacts the gas distribution valve backward, and then the upper shaft sleeve breaks rocks above the DTH hammer to help in releasing the sticking drilling tools. According to the structure and operating principle of the bidirectional pneumatic DTH hammer, a physical model was established based on the pneumatic transmission theory. With the SimulationX software, a simulation model was constructed using pneumatic transmission module components. The velocities, displacements, and impact energy of the piston were analyzed, with several main factors being considered including piston mass, the total weight of the DTH hammer, compressed air pressure, and the lifting distance of the inner tube assembly. From the analysis results, an increase in piston mass leads to a decrease in the piston impact frequency and peak impact velocity, but the results show a negligible effect on impact energy. As the total weight of the DTH hammer changes, there is little variation in the piston impact frequency, peak impact velocity, piston displacement, and piston impact energy. While increasing the gas source pressure, the piston impact frequency, peak of impact velocity, velocity

reduction amplitude, piston upward end point, and piston impact energy all increase. For the backward impact process, as the lifting distance increases, the peak impact velocity increases, thereby increasing the acceleration distance. Therefore, a piston mass of 18 kg, total weight of 125 kg, gas source pressure of 2.2 MPa, and lifting distance of 60 mm for the backward impact were recommended. To verify the operating performance of the DTH hammer, a set of bidirectional pneumatic DTH hammers were manufactured and tested in gravel formations. During the experiments, the bidirectional DTH hammer was in good working condition. The maximum drilling rate can reach up to 1.5 m/min, and the actual bit on the bottom time was much shorter than the auxiliary time of adding drill pipes. By lifting the DTH hammer away from the bottom of the borehole and pumping compressed air, the DTH hammer piston can achieve a high frequency backward impact. There are no drilling tools' sticking or burying accidents. The above results indicated that the bidirectional pneumatic DTH hammer can effectively form boreholes in loose formations and deal with drilling tools' sticking or burying accidents.

Author Contributions: Methodology, Y.S.; software, Y.S. and C.L.; investigation, Y.S. and S.H.; writing—original draft preparation, Y.S. and S.H.; writing—review and editing, Y.S. and S.H.; project administration, Y.S.; funding acquisition, Y.S. All authors have read and agreed to the published version of the manuscript.

Funding: This research was funded by Natural Science Foundation of Anhui Province (2108085QE210), Natural Science Foundation of the Anhui Higher Education Institutions (KJ2019A0102), Academician Workstation in Anhui Province, Anhui University of Science and Technology (2022-AWAP-05), Major science and technology projects in Anhui Province (202203a07020009, 201903a05020012), and Scientific Research Foundation of AUST.

Institutional Review Board Statement: Not applicable.

Informed Consent Statement: Not applicable.

Data Availability Statement: Not applicable.

Conflicts of Interest: The authors declare no conflict of interest.

References

1. Zhao, X.; Qiu, Z.; Wang, M.; Xu, J.; Huang, W. Experimental investigation of the effect of drilling fluid on wellbore stability in shallow unconsolidated formations in deep water. *J. Pet. Sci. Eng.* **2019**, *175*, 595–603. [CrossRef]
2. Akl, S.; Whittle, A. Stability analyses for deviated wellbores in unconsolidated cross-anisotropic formations. *Can. Geotech. J.* **2016**, *53*, 1450–1459. [CrossRef]
3. Van der Schans, M.; Bloemendal, M.; Robat, N.; Oosterhof, A.; Stuyfzand, P.; Hartog, N. Field Testing of a Novel Drilling Technique to Expand Well Diameters at Depth in Unconsolidated Formations. *Groundwater* **2022**, *60*, 808–819. [CrossRef] [PubMed]
4. Hou, B.; Zeng, C.; Chen, D.; Fan, M.; Chen, M. Prediction of Wellbore Stability in Conglomerate Formation Using Discrete Element Method. *Arab. J. Sci. Eng.* **2017**, *42*, 1609–1619. [CrossRef]
5. Liu, D.; Han, L.; Yang, P. Research on Mechanism of Wellbore Instability in Gravel Formations during Air Drilling and Application. *Drill. Prod. Technol.* **2019**, *42*, 5–8. (In Chinese)
6. Gao, K.; Liu, J.; Chen, H.; Li, X.; Huang, S. Dynamic Characteristics of Rock Holes with Gravel Sediment Drilled by Bit Anchor Cable Drilling. *Sustainability* **2023**, *15*, 5956. [CrossRef]
7. Kumar, A.; Samuel, R. Analytical Model to Characterize 'Smear Effect' Observed While Drilling with Casing. *J. Energy Resour. Technol.-Trans. ASME* **2014**, *136*, 033101. [CrossRef]
8. Kondratenko, A.; Shakhtorin, I. Engineering solutions for casing drilling in pre-mine drainage. *IOP Conf. Ser. Earth Environ. Sci.* **2019**, *262*, 012031. [CrossRef]
9. Sánchez, F.; Al-Harthy, M. Risk analysis: Casing-while-Drilling (CwD) and modeling approach. *J. Pet. Sci. Eng.* **2011**, *78*, 1–5. [CrossRef]
10. Cao, P.; Cui, G.; Qi, B.; Yao, S.; Zheng, Z.; Bo, K. Investigation on the cuttings carrying capacity of a novel retractable drill bit used in casing while drilling with air reverse circulation. *J. Pet. Sci. Eng.* **2022**, *219*, 111079. [CrossRef]
11. Cirimello, P.; Otegui, J.; Carfi, G.; Morris, W. Failure and integrity analysis of casings used for oil well drilling. *Eng. Fail. Anal.* **2017**, *75*, 1–14. [CrossRef]
12. Timonin, V.; Alekseev, S.; Karpov, V.; Chernienkov, E. Influence of DTH Hammer Impact Energy on Drilling-with-Casing System Performance. *J. Min. Sci.* **2018**, *54*, 53–60. [CrossRef]

13. Sanchez, F.; Turki, M.; Nabhani, Y.; Cruz, M.; Houqani, S. Casing While Drilling (CwD): A New Approach to Drilling Fiqa Formation in the Sultanate of Oman-A Success Story. *Spe Drill. Complet.* **2012**, *27*, 223–232. [CrossRef]
14. Qi, B.; Cao, P.; Yang, H.; He, W.; Wang, M.; Chen, B.; Bo, K.; Zheng, Z. Experimental and Numerical study on Air Flow Behavior for a Novel Retractable Reverse Circulation Drill Bit of Casing-while-Drilling (CwD). *Geofluids* **2021**, *2021*, 3586572. [CrossRef]
15. Liu, L.; Zhou, J.; Kong, L.; Wang, Y.; Li, J. Analysis of the dynamic response and impact parameters of pneumatic down-the-hole hammer drilling rescue holes. *Geoenergy Sci. Eng.* **2023**, *228*, 211935. [CrossRef]
16. Bo, K.; Sun, S.; Hu, Y.; Wang, M. Design Optimization and Performance Analysis of the Pneumatic DTH Hammer with Self-Propelled Round Bit. *Shock Vib.* **2021**, *2021*, 6653390. [CrossRef]
17. Zhao, Z.; Meng, Y.; Li, Y.; Shi, X.; Xiang, C. Effects of Working Angle on Pneumatic Down-the-hole Hammer Drilling. *Rock Mech. Rock Eng.* **2015**, *48*, 2141–2155. [CrossRef]
18. Li, Y.; Peng, J.; Huang, C.; Lian, M.; Xu, T.; Zhang, Y.; Bo, K.; Feng, B.; Zhou, J. Multi-fractured stimulation technique of hydraulic fracturing assisted by the DTH-hammer-induced impact fractures. *Geothermics* **2019**, *82*, 63–72. [CrossRef]
19. Ge, D.; Peng, J.; Li, K.; Huang, C.; Lian, M.; Yang, Z. Influence of water-based drilling fluids on the performance of the fluidic down-the-hole hammer. *J. Pet. Sci. Eng.* **2020**, *195*, 107817. [CrossRef]
20. Wu, T.; Tang, Y.; Tang, S.; Li, Y.; He, W.; Chen, E. Design and analysis of a new down-the-hole electromagnetic hammer driven by tube linear motor. *IET Electr. Power Appl.* **2017**, *11*, 1558–1565. [CrossRef]
21. Kim, D.; Oh, J.; Cho, J.; Kim, J.; Chung, J.; Song, C. Design study of impact performance of a DTH hammer using PQRSM and numerical simulation. *J. Mech. Sci. Technol.* **2019**, *33*, 5589–5602. [CrossRef]
22. Zhang, X.; Luo, Y.; Fan, L.; Peng, J.; Yin, K. Investigation of RC-DTH air hammer performance using CFD approach with dynamic mesh method. *J. Adv. Res.* **2019**, *18*, 127–135. [CrossRef] [PubMed]
23. Kim, D.; Kim, J.; Lee, B.; Shin, M.; Oh, J.; Cho, J.; Song, C. Prediction model of drilling performance for percussive rock drilling tool. *Adv. Civ. Eng.* **2020**, *2020*, 8865684. [CrossRef]
24. Wang, Y.; Quan, Q.; Yu, H.; Bai, D.; Li, H.; Deng, Z. Rotary-percussive ultrasonic drill: An Effective subsurface penetrating tool for minor planet exploration. *IEEE Access* **2018**, *6*, 37796–37806. [CrossRef]
25. Zhukov, I.; Smolyanitsky, B.; Timonin, V. Improvement of Down-the-Hole Air Hammer Efficiency by Optimizing Shapes of Colliding Parts. *J. Min. Sci.* **2018**, *54*, 212–217. [CrossRef]
26. He, J.; Zhao, Z.; Yin, Q.L.; Luo, Y.; Gan, X. Design and optimisation on rapid rescue well-drilling technology with large-diameter pneumatic hammers. *Int. J. Min. Reclam. Environ.* **2019**, *34*, 19–33. [CrossRef]

Disclaimer/Publisher's Note: The statements, opinions and data contained in all publications are solely those of the individual author(s) and contributor(s) and not of MDPI and/or the editor(s). MDPI and/or the editor(s) disclaim responsibility for any injury to people or property resulting from any ideas, methods, instructions or products referred to in the content.